Arnold Tongue of Electrochemical Nonlinear Oscillators

Satoshi Nakata,*,†,‡ Kazuya Miyazaki,‡ Suguru Izuhara,‡ Hirokazu Yamaoka,§ and Dan Tanaka||,⊥

Graduate School of Science, Hiroshima University, Kagamiyama 1-3-1, Higashi-Hiroshima 739-8526, Japan, Department of Chemistry, Nara University of Education, Takabatake-cho, Nara 630-8528, Japan, Graduate School of Engineering, University of Fukui, 3-9-1 Bunkyo, Fukui 910-8507, Japan, Department of Complex Systems Science, Graduate School of Information Science, Nagoya University, Furo-cho, Chikusa-ku, Nagoya, 464-8601, Japan, and PRESTO, Japan Science and Technology Agency, 4-1-8, Honcho Kawaguchi, Saitama, 332-0012, Japan

Received: March 2, 2009; Revised Manuscript Received: May 10, 2009

We study the Arnold tongue of a nonlinear electrochemical oscillator entrained to an electrical periodic forcing. In our system, the width of the 1:3 entrainment region was broader than that of the 1:2 region. The 1:1 and 1:3 regions became monotonically broad when the conductance of the electrode cell was increased by the electrochemical redox reaction of $Fe(CN)_6^{4-} \rightleftarrows Fe(CN)_6^{3-} + e$. In contrast, the 1:2 region changed nonmonotonically. In particular, the rate of change in the 1:2 region was greater than those of the 1:1 and 1:3 regions. These experimental results were qualitatively reproduced by the use of phase response curves of a corresponding mathematical model. We also discuss higher harmonics included in a limit cycle describing the isolated oscillator, dependence on the redox reaction, and hysteresis due to a bistability.

1. Introduction

When two or more nonlinear oscillators are coupled together, the phases of the oscillators can be locked at a constant value. This phenomenon is called "synchronization" and is one of the most interesting phenomenon observed in nonlinear systems.[1,2] Synchronization is widely observed in living organisms, such as in the beating heart, circadian rhythm, the organized rhythm in the flashing of swarms of fireflies, and so on.[3,4] There have also been many experimental and theoretical studies on the synchronization of physicochemical coupled oscillators. For example, a synchronized chemical wave among small beads[5] or stirred containers[6] has been reported using the Belousov−Zhabotinsky reaction. Hudson and coworkers reported the synchronization of electrochemical oscillations on electrode arrays.[7,8] The coupling of salt-water oscillators, which were constructed by two or three cups of salt water connected to a larger vessel of pure water through a small orifice at the bottom of the individual cups, exhibited various features of synchronization.[9−12] Two camphor boats exhibited synchronized sailing on a water chamber as an autonomous system.[13]

Synchronization to an external force is called "entrainment". The parameter region in which the entrainment is exhibited is called an "Arnold tongue" because the shape of the parameter region is an upside-down triangle and is similar to a tongue. To recognize Arnold's enormous contribution to the study of entrainments, this tongue is called the Arnold tongue in several research fields.[14−16] In this article, we report a coupled system with a nonlinear chemical oscillator and an external force, which can serve as a simple system for studying entrainment. Here the nonlinear chemical oscillator is composed of a Wien bridge circuit in an electrochemical cell.[17−19] The advantage of this system is that it is easy to control the experimental parameters, for example, amplitude and frequency of the oscillation, and to simulate the circuit numerically. In our system, a nonlinear chemical oscillator with an electrochemical cell is entrained by the external forcing of electric circuits in some parameter regions. In particular, the parameter region of 1:2 entrainment, where 1:2 is the ratio of the frequency of the chemical oscillator to that of the external forcing, is remarkably narrow for an inorganic aqueous solution without an electrochemical redox reaction. With the addition of an electrolyte that generated the electrochemical redox reaction, the parameter region of 1:2 entrainment was increased, and hysteresis between 1:1 and 1:2 entrainment was observed. These experimental results were qualitatively reproduced by theoretical models.

2. Experiments

The experimental apparatus is shown schematically in Figure 1. A Wien bridge oscillator, which consisted of an operational amplifier, was generally used as a linear oscillator; that is, the waveform of the Wien bridge oscillator was sinusoidal (Figure 1a). If the sinusoidal voltage of an external force (V_1) is applied to a "linear" Wien bridge circuit (V_2), then the V_1 versus V_2 curve is usually not given by a closed line because the frequencies of the individual oscillators are independent. When an electrochemical cell is connected to a Wien bridge circuit in place of a parallel circuit for the standard "linear" capacitance (C_s) and standard "linear" resistance (R_s), the waveform is deformed from a sinusoidal wave because an electrochemical system is generally nonlinear (Figure 1b).[17−19] For the electrochemical cell, two electrodes, a platinum disk (diameter: 6 mm), and a platinum wire (length 20 mm, diameter 0.5 mm) were immersed in a test aqueous solution (20 mL) with stirring, and the platinum wire was connected to the ground. Sinusoidal voltage of the external force ($V_1 = E_1 \cos 2\pi f_1 t$, V) was generated with a waveform generator (model 1920A, NF

* To whom correspondence should be addressed. Tel/Fax: +81-82-424-7409. E-mail: nakatas@hiroshima-u.ac.jp.
† Hiroshima University.
‡ Nara University of Education.
§ University of Fukui.
|| Nagoya University.
⊥ Japan Science and Technology Agency.

10.1021/jp9020189 CCC: $40.75
Published on Web 06/02/2009

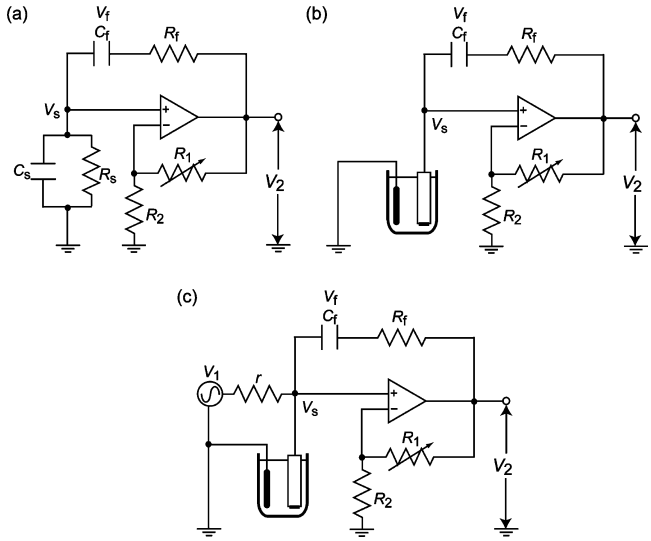

Figure 1. Schematic illustration of (a) the Wien bridge oscillator in general, (b) the Wien bridge circuit connected to the electrochemical cell in place of the parallel circuit for the standard "linear" capacitance (C_s) and standard "linear" resistance (R_s) (Wien bridge nonlinear oscillator), and (c) the coupling system between the forced oscillator (linear oscillator, V_1) and the Wien bridge nonlinear oscillator (V_2) via resistance, r. The relationship between V_1 and V_2 was observed in the entrainment. $C_f = 4.7\ \mu$F, $R_f = 100$ kΩ, $R_2 = 3.3$ kΩ, and $r = 100$ kΩ.

Electronics Instruments, Japan) and applied to the test solution via resistance, r (Figure 1c). Here r corresponded to the coupling strength; that is, the voltage of the Wien bridge oscillator, V_2, was easily influenced by V_1 when r was low and vice versa. An LF356H was used as an operational amplifier. The sinusoidal voltage and the voltage of the oscillations were recorded by a personal computer. All chemicals were purchased from Sigma-Aldrich (St. Louis, MO). Water was deionized with ion-exchange resin, distilled, and then purified with a Millipore Milli-Q filtering system. All measurements were performed at 298 ± 1 K.

3. Experimental Results

Figure 2 shows (a) a mode-locking diagram on the (f_1, E_1) plane for 0.2 M Na_2SO_4 aqueous solution with or without 0.25 mM $K_4Fe(CN)_6$ as an electrochemical redox reaction and (b) typical features of entrainment by using the experimental system in Figure 1c.

The Wien bridge oscillator with the electrode cell was clearly nonlinear because the V_1 versus V_2 curve was characteristically deformed from an ellipsoid or line; that is, the time variation of V_2 was deformed from a sinusoidal wave, as shown in Figure 2b. For the region of entrainment, the V_1 versus V_2 curve was closed within 1 min and maintained for at least 50 cycles. In contrast, the V_1 versus V_2 curve was not closed for the region without entrainment.

With the addition of $K_4Fe(CN)_6$, the region of 1:1 ($= f_2/f_1$) entrainment did not change much, but the region of 1:2 entrainment was clearly increased, where f_2 is the frequency of V_2, that is, the frequency of the circuit. For the comparative experiments, the regions of 1:1, 1:2, and 1:3 entrainment did not change much with the addition of 0.25 mM KCl (data not shown). The regions of entrainment (1:1, 1:2, and 1:3) increased with an increase in E_1.

Hysteresis depending on the initial value of f_1 was observed in the region of coexistence of 1:1 and 1:2 entrainment, as seen

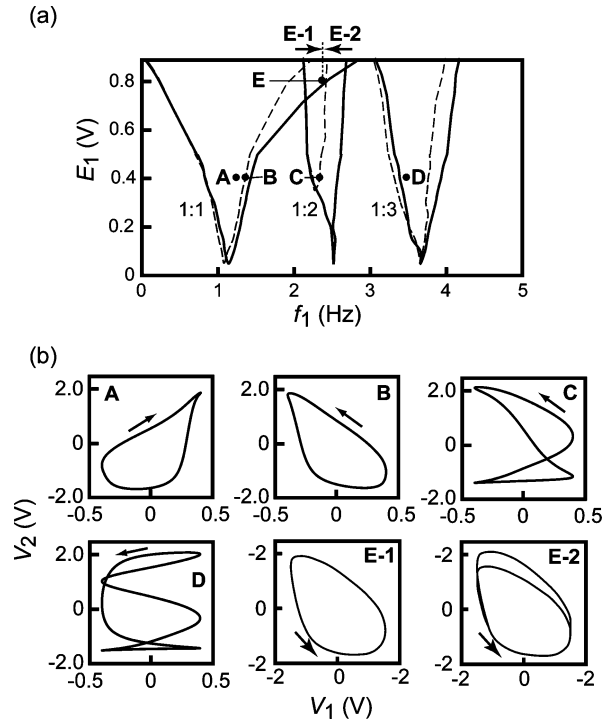

Figure 2. (a) Mode-locking diagram on the (f_1, E_1) plane in the electrochemical cell including 0.2 M Na_2SO_4 (---) and 0.2 M Na_2SO_4 plus 0.25 mM $K_4Fe(CN)_6$ (—). (b) Typical features of entrainment (1:1 (**A**, **B**), 1:2 (**C**), and 1:3 (**D**)) for $E_1 = 0.4$ V. The point **E** is $E_1 = 1.0$ V and $f_1 = 2.44$ Hz in the region of coexistence of 1:1 and 1:2 entrainment. **E-1** and **E-2** are the features of entrainment when the initial values of f_1 were 2 and 2.5 Hz, respectively. **A**−**E** in part b correspond to those in part a.

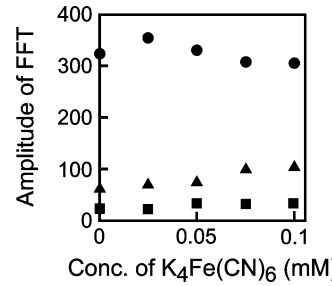

Figure 3. Amplitudes of FFT (●, fundamental harmonic; ▲, second harmonic; ■, third harmonic) for V_2 without the external force depending on the concentration of $K_4Fe(CN)_6$ in 0.2 M Na_2SO_4.

in point **E** in Figure 2a. In this experiment, f_1 was changed from an initial value to that in **E**. We observed 1:1 entrainment when the initial value of f_1 was lower than that in **E**. (See **E-1** in Figure 2b.) In contrast, 1:2 entrainment was observed when the initial value of f_1 was higher than that in **E**. (See **E-1** in Figure 2b.) These phenomena were not observed under the same E_1 and f_1 for 0.2 M Na_2SO_4 solution without $K_4Fe(CN)_6$.

Figure 3 shows the fundamental, second, and third harmonics of the amplitudes of FFT for V_2 without V_1 depending on the concentration of $K_4Fe(CN)_6$ in 0.2 M Na_2SO_4 to evaluate the waveform of V_2. The second harmonic increased with an increase in the concentration of $K_4Fe(CN)_6$ in comparison with the fundamental and third harmonics.

4. Discussion

The characteristic features of entrainment correspond to the voltage-dependent capacitance and voltage-dependent conductance. The regions of these entrainments change depending on

the nature of voltage-dependent conductance. In particular, the region of 1:2 entrainment increases with the addition of $K_4Fe(CN)_6$, as seen in Figure 2a. The addition of $K_4Fe(CN)_6$ clearly increases the conductance around $V = 0$; that is, it corresponds to the current generated by the electrochemical redox reaction of $Fe(CN)_6^{4-} \rightleftarrows Fe(CN)_6^{3-} + e$, such as in cyclic voltammetry.[20] When the same concentration of KCl was added to the test solution in place of $K_4[Fe(CN)_6]$, the region of 1:2 entrainment did not change. Although the conductance of the test solution increases with the concentration of inorganic ions, the slope of the current−voltage curve around $V = 0$ for the redox reaction is significantly higher than that for the addition of inorganic ions.[20] Figure 3 suggests that the increase in the second harmonic reflects the increase in the width of the 1:2 region with the addition of $K_4[Fe(CN)_6]$.

To clarify the physicochemical meaning of entrainment, we performed a numerical calculation for the Wien bridge oscillator with voltage-dependent capacitance (differential capacitance) and voltage-dependent conductance. The circuit used for the simulation is shown schematically in Figure 1a, and we suppose that the electrode cell is replaced by a parallel circuit that is composed of resistance and capacitance. (See Figure 1b.) The voltage and current in the circuit are described by the following differential equations.[17−19]

The equations for the voltage are

$$V_2 = V_s + V_f + R_f C_f \left(\frac{dV_f}{dt}\right) \quad (1)$$

$$V_2 = \frac{R_s + R_f}{R_2} V_s \quad (2)$$

The equation for the current is

$$\begin{aligned} C_f(dV_f/dt) &= V_s/R_s + dq_s/dt + (V_s - V_1)/r \\ &= V_s/R_s + C_s(dV_s/dt) + (V_s - V_1)/r \end{aligned} \quad (3)$$

If we assume that the charge q_s has a simple nonlinear form, then voltage-dependent capacitance, C_s, is expressed as

$$C_s(V_s) = dq_s/dV_s = C_0 + C_1 V_s + C_2 V_s^2 + C_3 V_s^3 \quad (4)$$

where C_0, C_1, C_2, and C_3 are constants. With regard to the effect of the current, the conductance, G_s ($= R_s^{-1}$), at the redox potential increases with an increase in the degree of the electrochemical redox reaction.

Equations 1−3 can be transformed to

$$dV_f/dt = (R_1 V_s/R_2 - V_f)/C_f R_f \quad (5)$$

$$C_s(V_s) dV_s/dt = [-G_s - 1/r + R_1/(R_f R_2)]V_s - V_f/R_f + V_1/r \quad (6)$$

Next, we explain these experimental results by means of the phase reduction methods.[2] The reduced model is

$$\begin{aligned} &d\psi/dt = 2\pi f - a + \Gamma(\psi) \\ &\Gamma(\psi) \equiv (n/f_1)^{-1} \int_0^{n/f_1} Z(at' + \psi) P(at' + \psi, t')\, dt' \\ &P(\phi, t) \equiv E_1 \cos(2\pi f_1 t)/r C_s(V_s(\phi)) \end{aligned} \quad (7)$$

where $\psi = \phi - at$ with $a = 2\pi f_1/n$ (ϕ: the phase of the oscillation of (V_f, V_s), n: an arbitrary natural number, f: the natural frequency exhibited by (V_f, V_s) without perturbation). Z represents an operator that projects the perturbation, P, onto the frequency $d\Psi/dt$ through the term Γ.[2,21] Z and Γ are 2π-periodic functions of Ψ. Roughly speaking, the phase ϕ plays a role similar to that of $\arctan(V_s/V_f)$.[2]

If $d\Psi/dt = 0$, then the electrochemical oscillator exhibits an angular frequency, a ($= d\phi/dt$), which represents 1:n entrainment. This condition, $d\Psi/dt = 0$, is satisfied if and only if the following inequalities are satisfied

$$\min \Gamma < a - 2\pi f < \max \Gamma \quad (8)$$

f and Γ are numerically derived from the original model eqs 5 and 6 with constant conductance, G_s. All of the parameter values correspond to the experimental values for 0.2 M Na_2SO_4 aqueous solution without $K_4Fe(CN)_6$: $C_0 = 0.02$ μF, $C_1 = 0$, $C_2 = 0.1$ F/V^2, $C_3 = 0$, $C_f = 4.7$ μF, $R_f = 20$ kΩ, $r = 0.1$ MΩ, $R_1/R_2 = 4.0$, and $G_s = 74$ $\mu\Omega^{-1}$.

Figure 4 shows the parameter regions of (f_1, E_1) where the inequalities of eq 8 are satisfied within inverted triangles; that is, this figure shows 1:n entrainment regions of the voltage of the Wien bridge nonlinear oscillator, V_2, and the sinusoidal voltage of the external forcing, $V_1 = E_1 \cos(2\pi f_1 t)$. The 1:2 region is the narrowest, and the 1:1 region is the broadest; that is, the entrainment regions observed in the experiments are qualitatively reproduced by the numerical model. In addition, the regions of coexistences of 1:1 and 1:2 entrainment that indicate hysteresis (Figure 2a, **E** in Figure 2b) are also generated by the numerical calculation ($E_1 = 0.3$ V and $f_1 = 2.7$ Hz).

Figure 5 shows the width of the 1:n region at $E_1 = 0.5$ V as a function of the parameter G_s. Here G_s in Figure 5 referred to the current−voltage curve for a reversible system such as $[Fe(CN)_6]^{2+} \rightleftarrows [Fe(CN)_6]^{3+} + e^-$ at the redox potential.[16] With an increase in G_s, the 1:1 and 1:3 regions become monotonically broad. In contrast, the width of the 1:2 region depended nonmonotonically on the conductance. For example, the increase in current at $V = 0$ causes an increase in the width of the 1:2 region if G_s changes from 100 to 110 μS in this experiment. In particular, the degree of the increase in the 1:2 width is relatively greater than those in the 1:1 and 1:3 widths for $100 < G_s(\mu S) < 110$.

In contrast, if G_s changes from 80 to 100 or from 110 to 120 μS, then the increase in current at $V = 0$ caused the decrease in the width of the 1:2 region. The experimental results correspond to the former case in the numerical calculation. This nonmonotonic relationship between the increase in current at $V = 0$ and that in the width of the 1:2 region is a difficult subject to be explained and can be a result of system-specific details.

These results agree qualitatively with those observed in the experiments. We conjecture that the fact that the 1:2 region is sensitive to a change in conductance reflects the high sensitivity of the second harmonic of the electrochemical oscillation (cf., Figure 3).

5. Conclusions

The widths of the 1:1, 1:2, and 1:3 regions in the experiments and the features of entrainment with the addition of $K_4Fe(CN)_6$

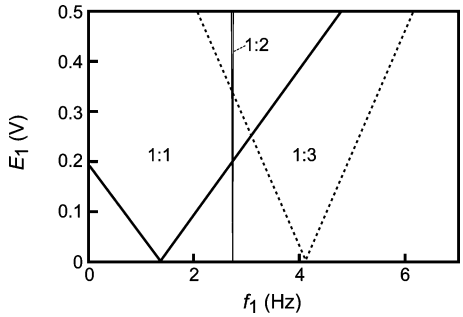

Figure 4. Numerical results in the regions of 1:*n* entrainment on the (f_1, E_1) plane based on eq 8.

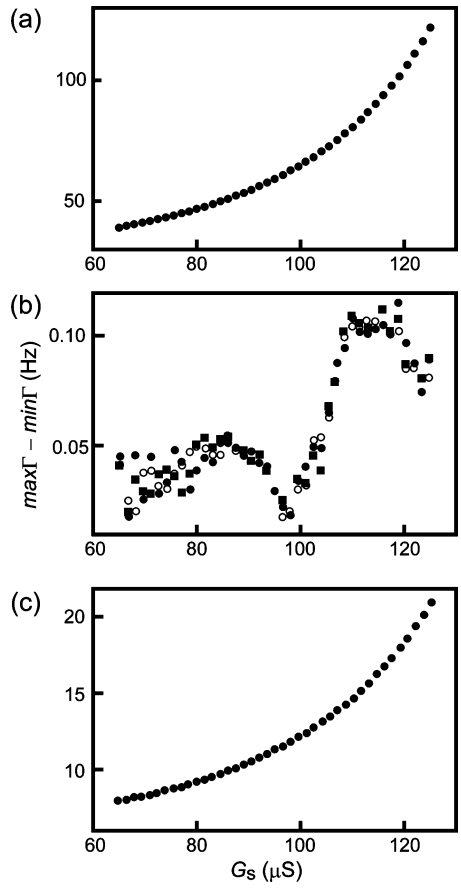

Figure 5. max Γ − min Γ as a function of the conductance, G_s, for (a) 1:1, (b) 1:2, and (c) 1:3 entrainment at $E_1 = 0.5$ V. In our numerical algorithm, we used a random variable. Each mark in the Figure corresponds to a trial with the random number.

were qualitatively reproduced by the numerical calculation. In addition, the experimental results of hysteresis between 1:1 and 1:2 entrainment were also reproduced by the numerical calculation. These numerical calculations were carried out using a theoretical model that was derived by means of phase reduction methods. Therefore, the electrochemical nonlinear response can be characterized by the use of entrainment, and the features of entrainment can be qualitatively addressed on the basis of the phase model. The quantitative reproducibility should be further considered to understand the features of entrainment and confirm the theoretical model in detail.

Using this strategy, various chemical compounds can be distinguished not only quantitatively but also qualitatively. The features of electrochemical "entrainment" have been shown to change characteristically depending on the chemical species, and information obtained from such "entrainment" can provide abundant information for chemical sensing.[17−19]

Acknowledgment. We thank Prof. Takashi Amemiya (Yokohama National University, Japan) for his helpful comments. The present study was supported by a Grant-in-Aid for Scientific Research (no. 20550124), by a grant from the Asahi Glass Foundation to S.N., and by a Grant-in-Aid for Young Scientists (B) (no. 20740221) from the Japan Society for the Promotion of Science to D.T.

Note Added after ASAP Publication. This article posted ASAP on June 2, 2009. Various corrections were made throughout the paper. The correct version posted on June 18, 2009.

References and Notes

(1) Pikovsky, A.; Rosenblum, M.; Kurths, J. *Synchronization: A Universal Concept on Nonlinear Sciences*; Cambridge University Press: Cambridge, 2001.
(2) Kuramoto, Y. *Chemical Oscillations, Waves, and Turbulence*; Springer: New York, 1984.
(3) Winfree, A. T. *The Geometry of Biological Time*; Springer: New York, 1980.
(4) Markus, M.; Kuschmitz, D.; Hess, B. *Biophys. Chem.* **1985**, *22*, 95.
(5) Nishiyama, N.; Eto, K. *J. Chem. Phys.* **1994**, *100*, 6977.
(6) Yoshimoto, M.; Yoshikawa, K.; Mori, Y. *Phys. Rev. E* **1993**, *47*, 864.
(7) Kiss, I. Z.; Wang, W.; Hudson, J. L. *J. Phys. Chem. B* **1999**, *103*, 11433.
(8) Zhai, Y.; Kiss, I. Z.; Hudson, J. L. *Ind. Eng. Chem. Res.* **2004**, *43*, 315.
(9) Nakata, S.; Miyata, T.; Ojima, N.; Yoshikawa, K. *Physica D* **1998**, *115*, 313.
(10) Miyakawa, K.; Yamada, K. *Physica D* **2001**, *151*, 217.
(11) Yoshikawa, K.; Oyama, N.; Shoji, M.; Nakata, S. *Am. J. Phys.* **1991**, *59*, 137.
(12) Das, A. K.; Srivastava, R. C. *J. Chem. Faraday Trans.* **1993**, *89*, 905.
(13) Nakata, S.; Doi, Y.; Kitahata, H. *J. Phys. Chem. B* **2005**, *109*, 1798.
(14) Arnold, V. I. *Trans. Am. Math. Soc., Series 2* **1965**, *46*, 213.
(15) Arnold, V. I. *Geometrical Methods in the Theory of Ordinary Differential Equations*; Levi, M., Ed.; Grundlehren der Mathematischen Wissenschaften, Vol. 250; Springer-Verlag: New York, 1983.
(16) Mori, H.; Kuramoto, Y. *Dissipative Structures and Chaos*; Springer-Verlag: New York, 1997.
(17) *Chemical Analysis Based on Nonlinearity*; Nakata, S., Ed.; NOVA: New York, 2003.
(18) Nakata, S.; Yoshikawa, K.; Kawakami, H. *Physica D* **1992**, *59*, 169.
(19) Nakata, S.; Izuhara, S.; Masui, K.; Islam, M. R. *Int. J. Unconventional Computing* **2009**, *5*, 39.
(20) Bard, A. J.; Faulkner, L. R. *Electrochemical Methods*; Wiley: New York, 1980.
(21) Ermentrout, B. *Neural Comput.* **1996**, *8*, 979.

JP9020189